THE JOURNAL OF PHYSICAL CHEMISTRY B

Article

pubs.acs.org/JPCB

Electrochemical Properties of the Double Layer of an Ionic Liquid Using a Dimer Model Electrolyte and Density Functional Theory

Douglas Henderson*,† and Jianzhong Wu*,‡

†Department of Chemistry and Biochemistry, Brigham Young University, Provo, Utah 84602-5700, United States

‡Department of Chemical and Environmental Engineering, University of California, Riverside, California 92521-0425, United States

ABSTRACT: Most theoretical studies of the properties of an electrolyte, including an ionic liquid, treat the electrolyte as a mixture of charged hard spheres in a solvent modeled as a dielectric continuum. However, ionic liquids generally consist of nonspherical ions that are not dissolved in a solvent. A simple extension of the primitivel model of electrolytes is to represent an ionic liquid as a mixture of charged hard spheres (negative monovalent ions in our case) and nonspherical ions consisting of a dimer of two touching hard spheres, one of which is charged (monovalent and positive in our case) and the other is neutral. This simple model has been used previously by Federov et al. and by ourselves. Here, we use the classical density functional theory to study the interfacial properties of the model ionic liquid over a range of electrode charges and two electrolyte concentrations. For simplicity, all of the spheres have the same diameter. In contrast to the simulations of Federov and Kornyshev, we find that a plot of the differential capacitance of the dimer electrolyte versus the surface potential typically exhibits only a single hump. Also, differing from the studies of Lamperski et al. for a spherical electrolyte, which showed a decline of the maximal differential capacitance as the ionic concentration decreases, the maximum of the differential capacitance of the dimer electrolyte increases slightly with decreasing ionic concentration. Our theoretical results show other unexpected effects of the geometry of ionic species on the electrochemical properties of the electric double layer of an ionic liquid.

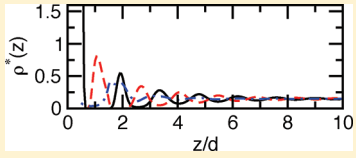

1. INTRODUCTION

There has been considerable work on the theory and simulations of the interfacial properties (the so-called double layer) of an electrolyte near a charged electrode. A recent review has been given by Henderson and Boda.[1] With little exception, these studies have been meant to describe the interfacial properties of aqueous electrolytes that exist at comparatively low ionic concentrations. The electrolyte may be represented by the primitive model; that is, the ionic solution is treated as a mixture of charged hard spheres in a dielectric continuum that represents the solvent. As was rightly pointed out by Kornyshev,[2] electrochemical properties of ionic liquids can be very different from those for aqueous electrolytes and deserve separate theoretical and experimental studies. Indeed, the primitive model is often not adequate for ionic liquids because they may not have a solvent and the organic ions are generally not spherical. In many cases, the electric double layers of ionic liquids are not even qualitatively described by the overused Gouy−Chapman theory.

Ionic liquids are of practical interest as environmentally friendly solvents for chemical reactions, for separation processes, and more recently for applications to a variety of energy devices including supercapacitors and lithium-ion batteries. Understanding the electrochemical properties of ionic liquids presents interesting challenges for both molecular simulation and theoretical modeling because of their strong electrostatic interactions, high ionic densities, and complicated ion geometry. While conventional models of electrolyte solutions are not directly applicable to ionic liquids, the simplicity and convenience of spherical ions make them popular among theoretical and simulation studies for the properties of ionic liquid double layers. For example, we note the simulations of Lamperski et al.[3−5] who studied the capacitance of the double layer formed by charged hard spheres near a hard planar charged surface. They found that, at low electrolyte concentration, the differential capacitance curve as a function of the electrode charge or potential had two humps, similar to a bactrian camel, with a minimum between the humps. Qualitatively, this is the situation for aqueous electrolytes. However, they found also that as the electrolyte concentration is increased, the minimum in the differential capacitance fills in, and, at high concentrations, the differential capacitance has a single hump, similar to a dromedary camel. In their study, the value of the differential capacitance at the minimum between the bactrian-like humps or at the maximum of the dromedary-like hump increases with increasing electrolyte concentration. As was pointed out by Kornyshev,[2] a single hump in the capacitance is typical of many ionic liquids. His theoretical predictions have been supported by the experimental work of Lockett et al.,[6] Islam et al.,[7,8] and Alam et al.[9] A hump in the differential capacitance curve has also been predicted by the modified Poisson−Boltzmann (MPB) theory[5] and implied by the mean-spherical approximation (MSA).[10] The density functional theory (DFT) study of Henderson et al.[11] is in very good agreement with the simulation results of Lamperski et al. The recent work of Loth et al.[12] presents an

Received: December 14, 2011
Revised: January 20, 2012
Published: January 26, 2012

   dx.doi.org/10.1021/jp212082k | J. Phys. Chem. B 2012, 116, 2520−2525

alternative theory and some simulations for the capacitance of a high density fluid near a polarizable metallic electrode.

A more realistic treatment of an ionic liquid would account for the ion geometry. Toward that end, perhaps the simplest model is that proposed by Federov et al.[13] and by ourselves[14] in which one of the ions consists of two tangentially connected hard spheres, one of which is charged (positive and monovalent in this work, for definiteness) and the other is neutral. For simplicity, we assume that the anions can be represented by monovalent charged spheres and that all spherical particles have the same diameter. In addition, the electrode is modeled as a hard planar charged surface. The dielectric constant of the surface is assumed to be equal to that of the electrolyte. Thus, polarization effects are not considered.

Our goal in this study is to determine whether the maximal value of the capacitance increases with the density of the fluid and study whether the change in the shape of the capacitance versus electrode charge curve that is seen in the theory and simulation of double layers containing spherical ions remains true for the dimer model of the capacitance of an ionic liquid double layer.

2. MODEL

In this study, the interaction between the hard spheres of species i and j, whose centers are separated by the distance R, is given by

$$\beta u_{ij}(R) = \begin{cases} \infty, & R < d \\ Z_i Z_j l_B / R, & R \geq d \end{cases} \tag{1}$$

where $\beta = 1/(k_B T)$ with k_B and T being the Boltzmann constant and the absolute temperature, respectively. Parameter d stands for the diameter of the hard spheres, which is taken to be equal for all of the spheres. Throughout this work, we use $d = 4.25$ Å, which is reasonable for an ionic liquid and is often used in molecular simulations. The valences, Z_i, are +1 and 0 for the two spheres in the dimer cation and −1 for the spherical anion. The pairs of positive and neutral spheres are tethered to form dimers of touching spheres. Parameter $l_B = \beta e^2/4\pi\varepsilon_0$ is the Bjerrum length, which is equal to 556.92 Å, a value that corresponds to electrostatic interaction in a vacuum at 298.15 K and that is much greater than that for an aqueous electrolyte solution, e is the magnitude of the elementary charge, and ε_0 is the permittivity of the free space. The charges of the spheres are assumed to be located at their centers. The chosen value of l_B corresponds to room temperature with the environment of the ions having a dielectric constant, ε, of unity. Arguably, ε for the ionic liquid may well be a little larger, say 2. We will consider the effects of this possibility in a subsequent study.

The interaction of a sphere with the planar electrode is given by

$$\beta\psi_i(z) = \begin{cases} \infty, & z < d/2 \\ -(2\pi l_B Z_i \sigma/e)z, & z \geq d/2 \end{cases} \tag{2}$$

where z is the perpendicular distance of the center of the sphere from the electrode surface. The parameter σ is the surface charge density (C/m^2) of the electrode, which is assumed to be planar, smooth, and nonpolarizable. The electrode charge is located on the surface (i.e., zero skin depth). As we have pointed out, the electrode is assumed to have the same dielectric constant as the electrolyte.

The structure of the interface is described by the density profiles of the ions, $\rho_i(z)$, which gives the local density of the ions of species i as a function of distance from the surface z. Once they are determined, the local electrical potential is determined from

$$\varphi(z) = \frac{e}{\varepsilon_0} \sum_i Z_i \int_z^\infty dz'(z - z')\rho_i(z') \tag{3}$$

and the charge density of the interface is given by

$$\sigma = -e \sum_i Z_i \int_{d/2}^\infty dz' \rho_i(z') \tag{4}$$

Because of electrostatic neutrality, the charge density of the interface must be equal in magnitude, but opposite in sign, to the integrated charge density of the mobile ions. Otherwise, there would be an electric field infinitely far from the electrode. The values of $\rho_i(z)$ are such that $\rho_i(\infty) = \rho_i = N_i/V$, where N_i and V are the number of spheres of species i and the volume of the bulk system, respectively.

We use dimensionless units throughout this work: $\sigma^* = \sigma d^2/e$, $\varphi^*(z) = \beta e\varphi(z)$, and $\rho^*_i(z) = \rho_i(z)d^3$. Two bulk densities of ions, $\rho_i^* = 0.05$ and 0.15, have been considered. Because of the charge neutrality, the density of monomeric ions is the same as that of the charged or neutral ends of the dimers. The latter density is the value that is appropriate for an ionic liquid. The lower density was selected so that the effect of changing in the ionic density could be examined. The total densities of all of the spheres are $\rho^* = 0.15$ and 0.45, respectively.

Our theoretical investigations are focused on the ionic density profiles, $\rho_i(z)$, the charge density of the interface σ, and the surface electric potential $\varphi(0)$. Additionally, we report values for the integral capacitance:

$$C_I^* = \frac{\sigma^*}{\varphi^*(0)} \tag{5}$$

and differential capacitance:

$$C_D^* = \frac{\partial\sigma^*}{\partial\varphi^*(0)} \tag{6}$$

For the record, the reduced temperature is $T^* = d/l_B = 0.00763$. The system is at room temperature, but T^* is very small because $\varepsilon = 1$ in the absence of a solvent. We realize that the effective dielectric constant of the medium of the ionic liquid might be somewhat greater than unity, perhaps 2. Additionally, the sphere diameter might exceed 4.25 Å. This would lead to a higher value of T^*. The consequences of a greater value for the dimensionless temperature will be considered in a later work.

A delineation of the bounds of the aqueous electrolyte and ionic liquid regimes within the primitive and primitive-like models can be given only roughly because the bounds are parameter dependent. Experimentally, the concentration of an aqueous electrolyte is typically 0.1 M or even less. The concentration of an ionic liquid is of the order of 5 M. However, a translation into reduced densities depends on the ion diameter. An increase in the ion diameter by a factor of 2 increases the reduced density by a factor of 8. The densities chosen in this study are reasonable. The reduced temperature of an aqueous electrolyte is fairly large ($T^* \approx 0.6$) because of the dielectric constant of water (76.5). The reduced density of a molten salt is similar to that of an ionic liquid. The reduced temperature of a room temperature ionic liquid is about 76.5 times smaller ($T^* \approx 0.008$). Ionic liquids can be thought of as room temperature molten salts. Molten salts typically exist at

dx.doi.org/10.1021/jp212082k | J. Phys. Chem. B 2012, 116, 2520−2525

temperatures of about 10 times room temperature. This is still a very small reduced temperature. Hence, in theory, the difference between an ionic liquid and a molten salt may not be all that significant. Roughly speaking, we might say that for primitive-like models the aqueous electrolyte regime corresponds to reduced densities below 0.05 and a reduced temperature of 0.6 (or 0.15 for divalent ions). The ionic liquid regime corresponds to a reduced density of about 0.10−0.25 (depending on the ion diameter) and a reduced temperature of about 0.01 with molten salts having a similar density and a somewhat higher reduced temperature.

3. DENSITY FUNCTIONAL THEORY

The detailed equations for the DFT calculations have been reported in previous publications.[11,14−19] Briefly, we start with an analytical expression for the intrinsic Helmholtz energy F or, equivalently, the grand potential Ω, as a functional of the underlying density profiles designated as $\rho_i(\mathbf{r})$. For the ionic systems considered in this work, the grand potential and the intrinsic Helmholtz energy are connected via the Legendre transformation:

$$\Omega = F + \int d\mathbf{r} \sum_i [\psi_i(\mathbf{r}) - \mu_i]\rho_i(z) \tag{7}$$

where ψ_i and μ_i stand for the one-body external potential and the chemical potential of ionic species i, respectively.

Near a planar electrode represented by a charged hard wall, the electrical potential and the ionic density profiles vary only in the z direction, that is, in the direction perpendicular to the electrode surface. At equilibrium, the grand potential is minimized with respect to the ionic density profiles, leading to the Euler−Lagrange equation:

$$\rho_i(z) = \rho_i \exp\{-\beta Z_i e\varphi(z) + \beta\mu_i^{ex} - \delta\beta[F_{hs}^{ex} + F_{chain}^{ex} + F_{ec}^{ex}]/\delta\rho_i(z)\} \tag{8}$$

where μ_i^{ex} stands for the excess chemical potential of particle i in a reference bulk fluid, and F_{hs}^{ex}, F_{chain}^{ex}, and F_{ec}^{ex} account for, respectively, the intrinsic Helmholtz energy due to the ionic size, the dimer chain connectivity, and the electrostatic correlations. As detailed in a previous work,[14] F_{hs}^{ex} is represented by a modified fundamental measure theory,[20−22] F_{chain}^{ex} is from an extension of the thermodynamic perturbation theory for inhomogeneous systems,[23,24] and F_{ec}^{ex} is formulated in terms of a quadratic density expansion of the excess Helmholtz energy with respect to that of a uniform ionic system with the input of the direct correlation functions obtained from the MSA.[25,26]

Equation 8 may be understood as a generalization of the Boltzmann equation for ionic distributions. Unlike the conventional Boltzmann equation for charged systems, however, eq 8 indicates that the structure of an inhomogeneous ionic system depends upon, in addition to the electrostatic potential, the ionic excluded volume and electrostatic correlation effects. While both effects are ignored in the Gouy−Chapman theory, we expect that they are important for an ionic liquid because of higher ionic density and stronger electrostatic interaction in comparison to those for a typical aqueous electrolyte solution.

The Euler−Lagrange equation is numerically solved by the Picard iteration. In calculation of the charge distributions, we start with a prespecified surface electric potential, $\varphi(0)$, and an initial guess for the density profiles of all ionic species, $\rho_i(z)$. The reduced mean electric potential is then calculated by integration of the Poisson equation:

$$\varphi^*(z) = \varphi^*(0) + 4\pi l_B \sum_i [\int_z^\infty dz' z Z_i \rho_i(z') + \int_0^z dz' z' Z_i \rho_i(z')] \tag{9}$$

Equation 9 is equivalent to eq 3 but is a convenient form for our computation. From $\varphi^*(z)$, we generate a new estimate for the density profiles from eq 8. The iteration process continues until the convergence of the electric potential and all density profiles. As $\varphi^*(0)$ is our input variable, the calculation of $\varphi^*(0)$ from eq 3 provides a useful consistency check.

4. RESULTS

We calculated the density profiles, $\rho_i^*(z)$, and from these obtained σ^*, $\varphi^*(0)$ (as a consistency check), C_I^*, and C_D^* for a wide range of values of $\varphi^*(0)$ for $T^* = 4.25/556.92 = 7.631 \times 10^{-3}$ and $\rho_i^* = 0.05$ and 0.15. A plot of $\varphi^*(0)$ as a function of σ^* for $\rho_i^* = 0.15$ is shown in Figure 1. Within the numerical

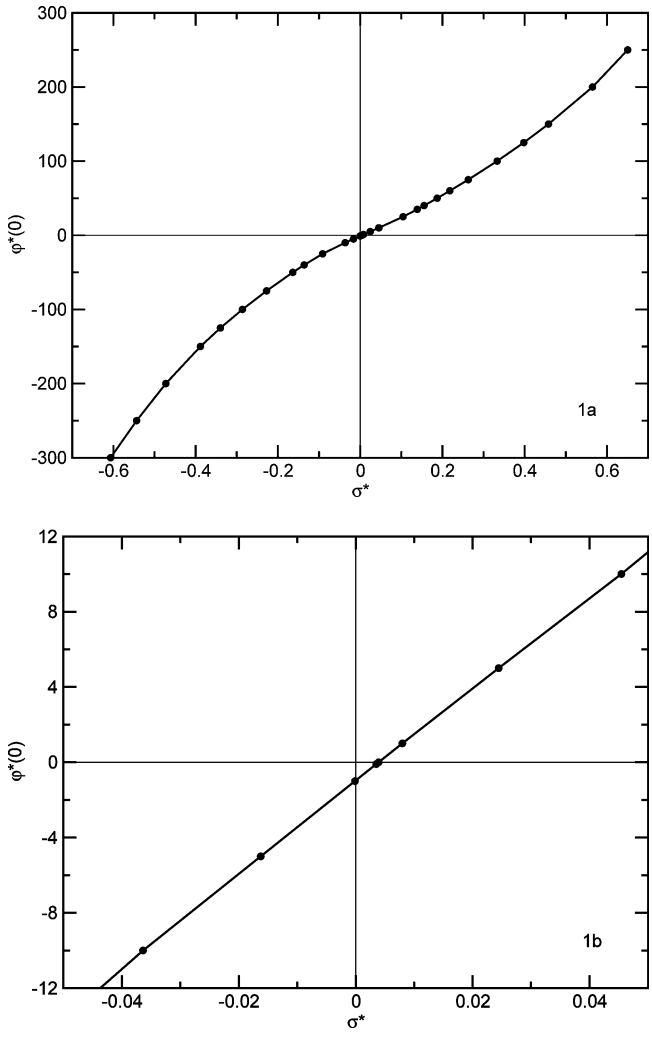

Figure 1. Dimensionless surface potential, $\varphi^*(0)$, as a function of the dimensionless surface charge density, σ^*, for $\rho_i^* = 0.15$. Part a gives results for a broad range of electrode charges, whereas part b focuses on the region of small electrode charge.

dx.doi.org/10.1021/jp212082k | J. Phys. Chem. B 2012, 116, 2520−2525

accuracy of our calculations, the potential at the PZC is $\varphi^*(0) = -1$ for both densities. The results for the two densities are little different for $\rho_i^* = 0.05$ even though the two cases differ by a factor of 3 in ionic density. Accordingly, only the results for $\rho_i^* = 0.15$ are shown in some of the following figures.

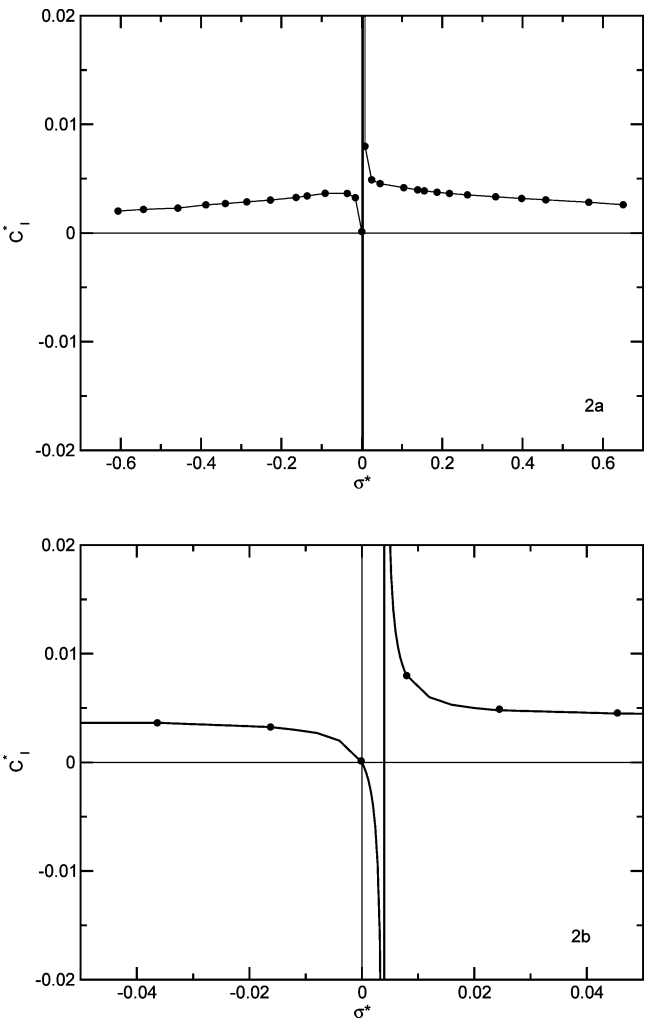

Figure 2. Dimensionless integral capacitance, C_I^*, as a function of the dimensionless surface charge density, σ^*, for $\rho_i^* = 0.15$. Part a gives results for a broad range of electrode charges, whereas part b focuses on the region of small electrode charge.

Figures 2 and 3 present, respectively, results for the integral and differential capacitances as functions of σ^* and $\varphi^*(0)$. While the differential capacitance of the dimer system is continuous and smooth, the integral capacitance is singular at the point of zero charge (PZC) where $\varphi^*(0) = 0$. In a symmetric electrolyte, both σ^* and $\varphi^*(0)$ vanish with a finite ratio at the PZC. In that case, the integral capacitance would be finite and smooth. Again, the conclusion is that there is little difference in the results for the capacitance for the two values of ρ_i^*. At both densities, the differential capacitance has bell or dromedary camel shape with a maximum at positive electrode charge, while the integral capacitance diverges at PZC. The value of the maximum in the differential capacitance decreases slightly when the density is increased.

The density profiles for $\rho_i^* = 0.15$ are plotted in Figure 4 for a positive, zero, and negative value of $\varphi^*(0)$ in parts a, b, and c,

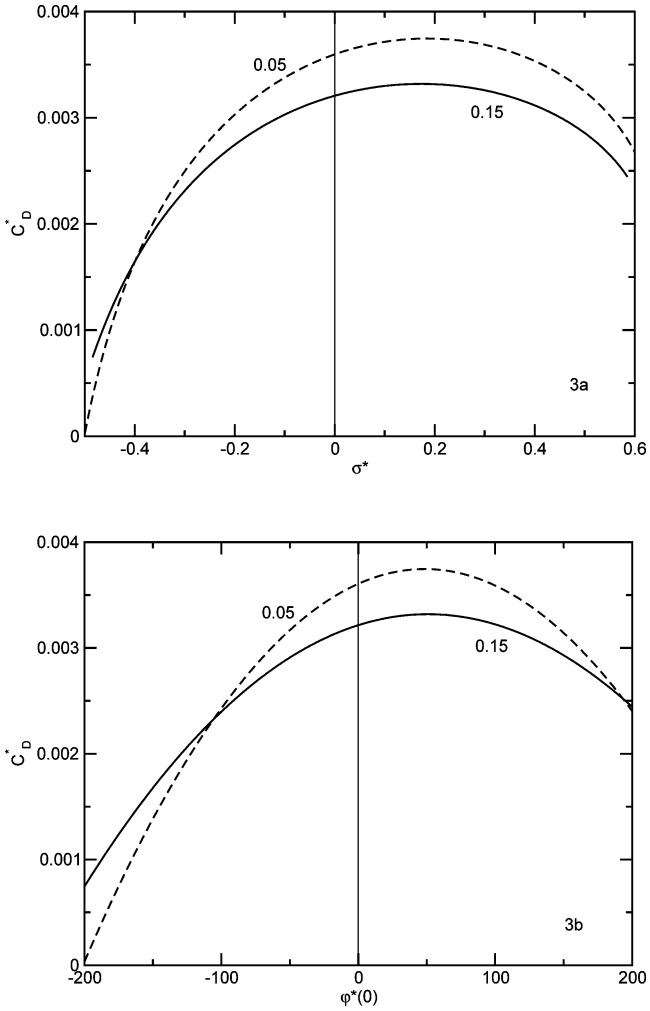

Figure 3. Dimensionless differential capacitance, C_D^* for $\rho_i^* = 0.05$ and 0.15. Parts a and b give the capacitance as a function of the dimensionless electrode charge density and electrode potential, respectively.

respectively. As expected, for the positive value of $\varphi^*(0) = 75$, part a, the negative ions approach the electrode more closely. The neutral end of the dimer tends to point toward the electrode but is pulled away by the positive end of the dimer that is repelled by the electrode. The profiles of the three species are more similar for part b. However, there is a slight positive surface charge for $\varphi^*(0) = 0$, and, as a result, there is a slight preference for negative ions to be near the electrode. The dimer seems to be nearly flat near the electrode. Further away from the electrode, the dimers tend to be oriented with the positive end further away from the electrode. Finally, when the electrode is negatively charged ($\varphi^*(0) = -75$, part c), the negative ion is repelled by the electrode, and many dimers are oriented with the positive end pointing to the electrode. However, there is an appreciable number of dimers whose neutral end is close to the electrode. This is because the positive end of the dimer is attracted by the negative ions that are away from the electrode.

A distinctive feature of ionic double layers is the pronounced oscillation in the ionic density profiles.[15] This long-range oscillation is missing in prediction of the Gouy−Chapman theory but has been confirmed by X-ray diffraction experiments.[27] It arises from the high density of the system and the strong electrostatic

dx.doi.org/10.1021/jp212082k | J. Phys. Chem. B 2012, 116, 2520−2525

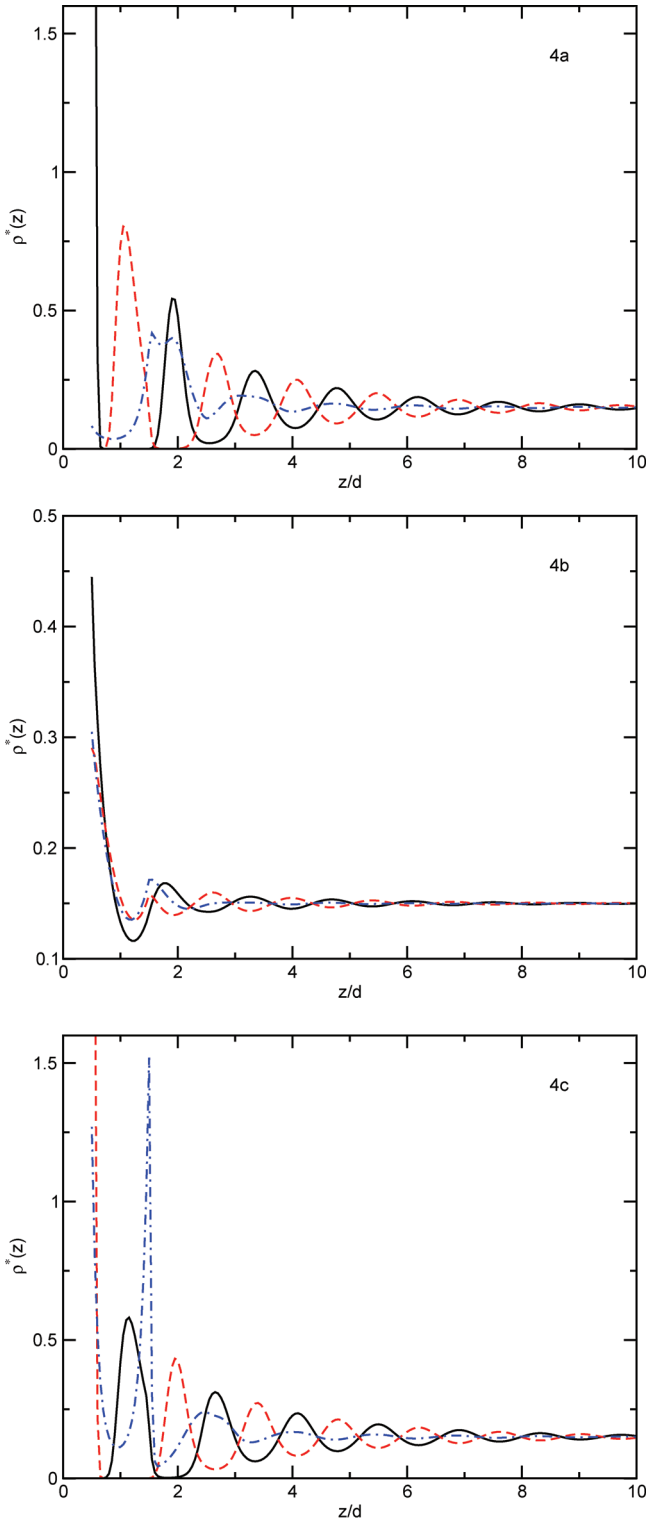

Figure 4. Ionic density profiles as a function of the normal distance from the electrode surface for $\rho_i^* = 0.15$. Parts a, b, and c give results for $\varphi^*(0) = 75$ ($\sigma^* = 0.263$), $\varphi^*(0) = 0$ ($\sigma^* = 0.004$), and $\varphi^*(0) = -75$ ($\sigma^* = -0.228$), respectively. The black (−), red (− − −), and blue (− · − · −) curves give the profiles for the spherical (negative) ions, the neutral spheres at one end of the dimer, and the positive spheres at the other end of the dimer, respectively.

forces and hard cores. The long-range oscillation of ionic density is most prominent for ionic liquids near highly charged electrodes.

5. SUMMARY AND DISCUSSION

We have presented DFT results for the surface potential $\varphi^*(0)$ as a function of charge density σ^* and the resultant capacitance curves for a model ionic liquid at the reduced densities $\rho_i^* = 0.05$ and $\rho_i^* = 0.15$. While the latter density is typical of an ionic liquid, we considered the lower density to examine the effect of the ion density on the differential and integral capacitances. Additionally, density profiles have been plotted for $\rho_i^* = 0.15$. The shape of the differential capacitance curve is nearly independent of ρ_i^* and, in this study, always has a bell (dromedary camel) shape. Also, the value of the maximum in the differential capacitance seems to decrease slightly with increasing ion density.

Our results are quite different from the situation for spherical ions as seen in the simulations and MPB study of Lamperski et al.[3−5] for spherical ions and our DFT study[11] for the same system, where the differential capacitance curve passes from a minimum at the PZC to maximum with a change in the shape of the curve from that of a bactrian to a dromedary camel and there is a uniform increase in the value of the differential capacitance at the PZC with increasing density. The increase in the capacitance with density is also seen in the MSA[10] and hypernetted chain approximation[28] for the system considered by Lamperski et al. Because the MSA is an analytic theory, it is easy to establish that an increase in the differential capacitance with increasing density is a general feature of the MSA for symmetric spherical ions.

It is interesting to note that in contrast to the study of Federov et al.[13] who found that the differential capacitance of a dimer (and trimer) model ionic liquid had a double hump (bactrian camel shape), only the monomer ionic fluid had a bell (dromedary camel) shape; we find that the differential capacitance of the dimer model ionic fluid has a bell shaped curve. Possibly, the answer to the question of whether the differential capacitance of a dimer model ionic liquid has a double hump or a bell shape is dependent upon the specific parameters of the system.

This study raises questions as well as answers. For example, what is the origin of the difference between the capacitance curve found here and that found by Federov et al.? Besides, simulation studies are needed to determine the accuracy of our DFT in the ionic liquid regime. We have made rapid progress in the development of a simulation code for a dimer system and expect to report results in the very near future.

AUTHOR INFORMATION

Corresponding Author

*E-mail: doug@chem.byu.edu (D.H.); jwu@engr.ucr.edu (J.W.).

Notes

The authors declare no competing financial interest.

ACKNOWLEDGMENTS

This work is in part supported by the National Science Foundation (NSF-CBET-0852353) and by the U.S. Department of Energy (DE-FG02-06ER46296).

REFERENCES

(1) Henderson, D.; Boda, D. *Phys. Chem. Chem. Phys.* **2009**, *11*, 3822−3830.
(2) Kornyshev, A. A. *J. Phys. Chem. B* **2007**, *111*, 5545−5557.

(3) Lamperski, S.; Outhwaite, C. W.; Bhuiyan, L. B. *J. Phys. Chem. B* **2009**, *113*, 8925−8929.
(4) Lamperski, S.; Henderson, D. *Mol. Simul.* **2011**, *37*, 264−268.
(5) Outhwaite, C. W.; Lamperski, S.; Bhuiyan, L. B. *Mol. Phys.* **2011**, *109*, 21−26.
(6) Lockett, R.; Sedev, R.; Ralston, J.; Horne, M.; Rodopoulos, T. *J. Phys. Chem. C* **2008**, *112*, 7486−7495.
(7) Islam, M. M.; Alam, M. T.; Ohsaka, T. *J. Phys. Chem. C* **2008**, *112*, 16568−16574.
(8) Islam, M. M.; Alam, M. T.; Okajima, T.; Ohsaka, T. *J. Phys. Chem. C* **2009**, *113*, 3386−3389.
(9) Alam, M. T.; Islam, M. M.; Okajima, T.; Ohsaka, T. *J. Phys. Chem. C* **2220**, *113*, 6596−6601.
(10) Henderson, D.; Lamperski, S.; Outhwaite, C. W.; Bhuiyan, L. B. *Collect. Czech. Chem. Commun.* **2010**, *75*, 303−312.
(11) Henderson, D.; Lamperski, S.; Jin, Z.; Wu, J. *J. Phys. Chem. B* **2011**, *115*, 12911−12914.
(12) Loth, M. S.; Skinner, B.; Shklovskii, B. I. *Phys. Rev. E* **2010**, *82*, 016107.
(13) Federov, M. V.; Georgi, N.; Kornyshev, A. A. *Electrochem. Commun.* **2010**, *12*, 296−299.
(14) Wu, J.; Jaing, T.; Jiang, D.; Zhehui, J.; Henderson, D. *Soft Matter* **2011**, *7*, 11222−11231.
(15) Wu, J. Z. *AIChE J.* **2006**, *52*, 1169−1193.
(16) Wu, J. Z.; Li, Z. D. *Annu. Rev. Phys. Chem.* **2007**, *58*, 85−112.
(17) Gillespie, D.; Valiskó, M.; Boda, D. *J. Phys.: Condens. Matter* **2005**, *17*, 6609−6626.
(18) Forsman, J.; Woodward, C. E.; Trulssonm, M. *J. Phys. Chem. B* **2011**, *115*, 4606−4612.
(19) Jiang, D. E.; Meng, D.; Wu, J. Z. *Chem. Phys. Lett.* **2011**, *504*, 153−158.
(20) Rosenfeld, Y. *Phys. Rev. Lett.* **1989**, *63*, 980−983.
(21) Yu, Y. X.; Wu, J. Z. *J. Chem. Phys.* **2002**, *117*, 10156−10164.
(22) Roth, R.; Evans, R.; Lang, A.; Kahl, G. *J. Phys.: Condens. Matter* **2002**, *14*, 12063−12078.
(23) Yu, Y. X.; Wu, J. Z. *J. Chem. Phys.* **2002**, *117*, 2368−2376.
(24) Li, Z. D.; Wu, J. Z. *Phys. Rev. Lett.* **2006**, *96*, 048302.
(25) Yu, Y. X.; Wu, J. Z.; Gao, G. H. *J. Chem. Phys.* **2004**, *120*, 7223−7233.
(26) Blum, L. *Mol. Phys.* **1975**, *30*, 1529−1535.
(27) Mezger, M.; Schroder, H.; Reichert, H.; Schramm, S.; Okasinski, J. S.; Schoder, S.; Honkimaki, V.; Deutsch, M.; Ocko, B. M.; Ralston, J.; Rohwerder, M.; Stratmann, M.; Dosch, H. *Science* **2008**, *322*, 424−428.
(28) Woelki, S.; Henderson, D. *Condens. Matter Phys.* **2011**, *14*, 43801.